Clim. Past, 17, 2165–2177, 2021
https://doi.org/10.5194/cp-17-2165-2021

Climate of the Past
Open Access
EGU

Climatic variations during the Holocene inferred from radiocarbon and stable carbon isotopes in speleothems from a high-alpine cave

Caroline Welte[1,2], Jens Fohlmeister[3,4,5], Melina Wertnik[1,2], Lukas Wacker[1], Bodo Hattendorf[6], Timothy I. Eglinton[2], and Christoph Spötl[7]

[1]Laboratory of Ion Beam Physics, ETHZ, Otto-Stern Weg 5, 8093 Zurich, Switzerland
[2]Geological Institute, ETHZ, Sonnegstrasse 5, 8092 Zurich, Switzerland
[3]Potsdam Institute for Climate Impact Research, Telegrafenberg, 14473 Potsdam, Germany
[4]GFZ German Research Centre for Geosciences, Section "Climate Dynamics and Landscape Development", 14473 Potsdam, Germany
[5]Federal Office for Radiation Protection, Köpenicker Allee 120-130, 10318 Berlin, Germany
[6]Laboratory of Inorganic Chemistry, D-CHAB, ETHZ, Vladimir-Prelog Weg 1, 8093 Zurich, Switzerland
[7]Institute of Geology, University of Innsbruck, Innrain 52f, 6020 Innsbruck, Austria

Correspondence: Caroline Welte (cwelte@phys.ethz.ch) and Jens Fohlmeister (jens.fohlmeister@pik-potsdam.de)

Received: 27 August 2020 – Discussion started: 24 September 2020
Revised: 19 July 2021 – Accepted: 2 September 2021 – Published: 19 October 2021

Abstract. Rapid and continuous analysis of radiocarbon (^{14}C) concentration in carbonate samples at spatial resolution down to 100 µm has been made possible with the new LA-AMS (laser ablation accelerator mass spectrometry) technique. This novel approach can provide radiocarbon data at a spatial resolution similar to that of stable carbon (C) isotope measurements by isotope ratio mass spectrometry of micromilled samples and, thus, can help to interpret δ^{13}C signatures, which otherwise are difficult to understand due to numerous processes contributing to changes in the C-isotope ratio. In this work, we analyzed δ^{13}C and ^{14}C on the Holocene stalagmite SPA 127 from the high-alpine Spannagel Cave (Austria). Both proxies respond in a complex manner to climate variability. Combined stable carbon and radiocarbon profiles allow three growth periods characterized by different δ^{13}C signatures to be identified: (i) the period 8.5 to 8.0 ka is characterized by relatively low δ^{13}C values with small variability combined with a comparably high radiocarbon reservoir effect (expressed as dead carbon fraction, dcf) of around 60 %. This points towards C contributions of host rock dissolution and/or from an "old" organic matter (OM) reservoir in the karst potentially mobilized due to the warm climatic conditions of the early Holocene. (ii) Between 8 and 3.8 ka there was a strong variability in δ^{13}C with values ranging from −8 ‰ to +1 ‰ and a generally lower dcf. The δ^{13}C variability is most likely caused by changes in C exchange between cave air CO_2 and dissolved inorganic carbon in drip water in the cave, which are induced by reduced drip rates as derived from reduced stalagmite growth rates. Additionally, the lower dcf indicates that the OM reservoir contributed less to stalagmite growth in this period possibly as a result of reduced meteoric precipitation or because it was exhausted. (iii) In the youngest section between 3.8 and 2.4 ka, comparably stable and low δ^{13}C values, combined with an increasing dcf reaching up to 50 % again, hint towards a contribution of an aged OM reservoir in the karst. This study reveals the potential of combining high-resolution ^{14}C profiles in speleothems with δ^{13}C records in order to disentangle climate-related C dynamics in karst systems.

1 Introduction

Understanding the climate of the past is the key for understanding how climate and environment will change in the future. Insights into paleoclimate are gained through the study of archives with stalagmites being a prominent example for

a terrestrial archive. Stalagmites can grow continuously over thousands to tens of thousands of years (Cheng et al., 2016; Fairchild et al., 2006; Moseley et al., 2020). Caves hosting stalagmites are present on all continents except Antarctica, and uranium-series disequilibrium dating allows robust chronologies to be built (Cheng et al., 2013; Richards and Dorale, 2003; Scholz and Hoffmann, 2008). Trace-element and stable isotope data of stalagmites allow the reconstruction of climatic conditions in the past. For example, the oxygen isotope composition ($\delta^{18}O$) is generally interpreted as a combination of a temperature and a meteoric precipitation signal (Lachniet, 2009; Wackerbarth et al., 2010). The interpretation of the stable carbon isotope signature ($\delta^{13}C$), however, is more challenging since additional local effects, such as vegetation changes (e.g., Bar-Matthews et al., 1999; Denniston et al., 2007; Fohlmeister et al., 2020), the carbonate dissolution mechanism (e.g., Fohlmeister et al., 2010b; Lechleitner et al., 2016) and in-cave fractionation processes (e.g., Mattey et al., 2016; Spotl et al., 2005) may have an influence, and little is known about the relative magnitude of these processes. Besides the stable C isotopes, radiocarbon (^{14}C), decaying with a half-life of $\sim$ 5700 yr (Kutschera, 2013), can be a valuable tool in speleothem research (e.g., Bajo et al., 2017; Lechleitner et al., 2016). So far, this isotope has not been fully exploited in speleothem science, mostly due to the time-consuming sampling and processing as well as the comparably high costs associated with the analyses. However, recently both issues have been considerably improved by inventions (Welte et al., 2016a, b) and advances in laser ablation coupled to accelerator mass spectrometry (LA-AMS; Welte et al., 2017; Yeman et al., 2019), which can be well applied to carbonate material.

We investigated a stalagmite that grew in the Spannagel cave system (Tyrol, Austria; Spötl et al., 2004) by means of C-isotope systematics. This high-alpine cave system was investigated in many studies in the context of palaeoclimate and palaeoenvironmental research mostly using O isotopes and growth phases as proxies (e.g., Fohlmeister et al., 2013; Spötl and Mangini, 2010). The gneiss covering the cave-bearing marble contains interspersed fine-crystalline pyrite (Spötl et al., 2004) and is topped by a thin soil layer with sparse vegetation. It was hypothesized that the oxidation of pyrite contributes considerably to the dissolution of the host-rock marble and, hence, to the growth of stalagmites and flowstones, in particular during cold climate periods when there is no soil present at this high altitude (Spötl and Mangini, 2007). During some interglacials including the Holocene, when Alpine soils are present in the catchment of the cave's drip water, sulfide oxidation and soil-derived CO_2 may operate in tandem. Consequently, the stable C-isotope signal of stalagmites from this cave is expected to vary significantly.

The aim of this study is to gain deeper insights into the climatically driven C dynamics in this cave by high spatially resolved ^{14}C analyses of a Holocene stalagmite. This study takes advantage of the recently introduced method of LA-AMS (Welte et al., 2016a, b), which reaches a similar spatial resolution to micromilling for stable isotope analysis (e.g., Spötl and Mattey, 2006). Using the combined ^{14}C and $\delta^{13}C$ records measured in this study as well as the previously published $\delta^{18}O$ signal (Fohlmeister et al., 2013), we explore the key processes influencing the carbon isotope composition of speleothems in this cave and gain a better understanding of the potential and limits of ^{14}C analysis of carbonates using LA-AMS.

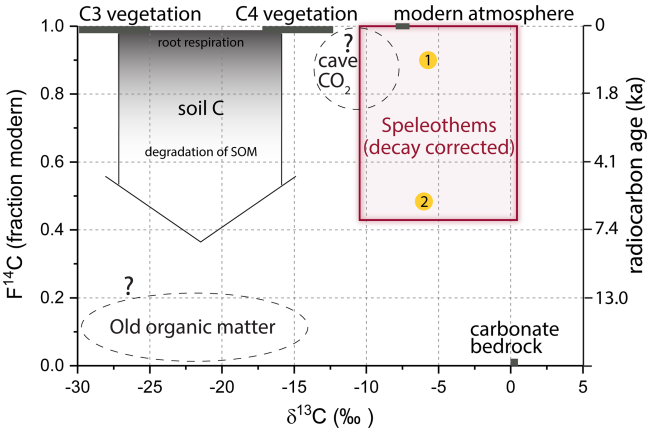

Figure 1. Carbon isotopic signatures of carbon-bearing reservoirs in karst systems. Yellow circles mark speleothem C resulting from different processes: (1) $CaCO_3$ dissolution via soil CO_2-derived carbonic acid; (2) deep organic carbon contribution to seepage water feeding speleothems (adapted from Fairchild and Baker, 2012).

2 Radiocarbon and dead carbon fraction

In most karst systems, dissolution of the carbonate host rock is driven by soil-derived carbonic acid forming in meteoric precipitation seeping through the soil. In this case, the two major soil-derived C sources contributing to the $\delta^{13}C$ values of the speleothem are pedogenic CO_2 from the degradation of soil organic matter (SOM, Trumbore, 2000) and root respiration (Cerling, 1984) that acidifies the meteoric water as it percolates through the soil. Recently, evidence was found for a potential additional C source stemming from CO_2 derived from the oxidation of "old" organic matter (OM) in the deep vadose zone (Bergel et al., 2017; Noronha et al., 2015). The water charged with carbonic acid then dissolves the host rock $CaCO_3$. In some karst systems, the oxidation of pyrite has shown to contribute to the acidification of the seepage water and hence to speleothem formation (e.g., Spötl et al., 2016). All of those C pools have different characteristics with respect to their stable and radioactive isotope signatures (Fig. 1).

When working with radiocarbon in speleothems it is important to determine the reservoir effect (Genty and Massault, 1997). If a radiocarbon-independent chronology for the

stalagmite exists, the reservoir effect, which is often termed dead carbon fraction (dcf), can be derived through comparison of the measured ^{14}C profile in the stalagmite ($F^{14}C_{stal}$) with the ^{14}C atmosphere's signature ($F^{14}C_{atm}$) of the same time (Genty and Massault, 1997):

$$\mathrm{dcf} = \left(1 - \frac{F^{14}C_{stal}}{F^{14}C_{atm}}\right) \cdot 100\,\%. \quad (1)$$

Values for dcf range from a few percent up to 70 % (Bajo et al., 2017; Southon et al., 2012) and commonly vary within a single speleothem with time (Bajo et al., 2017; Noronha et al., 2014; Therre et al., 2020). The magnitude of the dcf is influenced by multiple factors, such as the age of soil OM, contributing to soil gas CO_2 production (Fohlmeister et al., 2011b) and consequently altering the ^{14}C concentration in the stalagmite. Also the CO_2 partial pressure (pCO_2) in the soil plays an important role, with a complex relationship between the amount of soil gas pCO_2 and the dcf (Fohlmeister et al., 2011b). Additionally, the conditions of karst dissolution, i.e., open vs. closed system (Fohlmeister et al., 2011a; Hendy, 1971), affect the dcf. In a more open system, the dcf is low because the percolating water can continuously exchange C isotopes with the soil gas CO_2 leading to a ^{14}C concentration in the stalagmite that is dominated by the near-atmospheric soil ^{14}C signature (Southon et al., 2012). In a more closed system, this exchange is inhibited with the extreme case being a completely closed system, where for each mole of carbonic acid one mole of $CaCO_3$ is dissolved resulting in a dcf of up to 50 % (Hendy, 1971). Fractionation and C exchange between cave air CO_2 and dissolved inorganic carbon (DIC) in drip water are also potential candidates for modulation of the dcf. These main factors driving the dcf in turn are influenced by numerous parameters such as hydrological and environmental conditions above the cave. Several studies (e.g., Bajo et al., 2017; Fohlmeister et al., 2010; Griffiths et al., 2012; Lechleitner et al., 2016; Noronha et al., 2014) showed that during periods of increased rainfall the dcf in the stalagmite is enhanced. A likely explanation is a shift towards more closed-system conditions (Table 1) under higher meteoric precipitation regimes. It was argued that under more humid (arid) conditions the pore spaces in soils are clogged with (devoid of) water, leaving less (more) opportunity for C-exchange processes between dissolved inorganic C species and soil gas CO_2 (Fohlmeister et al., 2010).

An increasing number of cave systems have been reported where carbonate dissolution occurs even if no significant soil exists above the cave, indicating climatic conditions less suited for the existence of vegetation cover. Acidic conditions in the seepage water are achieved via oxidation of pyrite or other sulfide minerals disseminated in the bedrock (Bajo et al., 2017; Lauritzen, 2001; Spötl et al., 2016). In this case the C-isotope composition in the drip water is dominated by the bedrock, and the dcf is therefore expected to be relatively high (> 50 %). Under those conditions the $\delta^{13}C$ values of the speleothems reflect those of the (marine-derived) bedrock, i.e., are shifted closer to 0 ‰ compared to lower $\delta^{13}C$ values of speleothem $CaCO_3$ of around −12 ‰ to −10 ‰ for cave systems with a soil and vegetation cover. An overview of relevant processes as well as the resulting dcf and $\delta^{13}C$ is summarized in Table 1.

3 Materials and methods

3.1 Sample

Spannagel cave is located in the Tux Valley (47.08028° N, 11.67167° E; Zillertal Alps, western Austria) and opens at 2531 m above sea level. It forms a more than 12 km long system of galleries and short shafts, which developed in a Jurassic marble tectonically overlain by gneiss. This superposition not only allows for high-precision U-series dating of stalagmites due to their relatively high U contents, but also gives rise to carbonate dissolution via sulfuric acid stemming from pyrite oxidation. The thin alpine soil provides an additional pedogenic source of acidity, and the interplay between the two processes is reflected by highly variable stable C-isotope values as well as dcf in Spannagel speleothems. Stalagmite SPA 127 was found in the eastern part of the cave system, which was never ice-covered during the Holocene (Fohlmeister et al., 2013). The stalagmite grew from 8.45 to 2.24 ka with an average growth rate of 25 µm/a based on nine U–Th ages (Fohlmeister et al., 2013). There is no macro- and microscopic evidence for the existence of hiatuses in this specimen. Further evidence for the absence of hiatuses is provided by two additional speleothems, SPA 12 and SPA 128, from the same cave, and these are partly coeval with SPA 127. These additional speleothems have a higher dating density in parts, where SPA 127 has only a few radiometric U–Th dating points, and also do not show evidence of hiatuses (Fohlmeister et al., 2013). In combination with the well replicated stable O isotope signals we are confident that the growth of SPA 127 was not interrupted by hiatuses.

The 15 cm long polished slab of the stalagmite analyzed in this study was first used for stable oxygen and carbon isotope analysis where sampling was performed along the extension axis. For LA-AMS analysis, the same section was used but broken in two pieces at a distance from the top (dft) of approximately 10 cm, which will be referred to as "top piece" and "bottom piece".

Stable isotope analysis

Subsamples for stable carbon isotope analysis were micromilled at 100 µm increments and measured using an automated online carbonate preparation system linked to a triple collector gas source mass spectrometer (Delta^{plus}XL, ThermoFisher, Bremen, Germany) at the University of Innsbruck. Values are reported relative to the Vienna Pee Dee Belemnite standard. The long-term precision of the $\delta^{13}C$ values (1 standard deviation of replicate analyses) is 0.06 % (Spötl,

Table 1. Simplified summary of expected $\delta^{13}C$ (assuming C_3 vegetation cover) and dcf values in stalagmite $CaCO_3$ for different dominant processes. In many karst systems various combinations of these processes complicate the interpretation. This table is a compilation of data from Fohlmeister et al. (2011b), Spötl et al. (2016) and Therre et al. (2020).

Process		Expected $\delta^{13}C$ (‰)	Expected dcf (%)
Carbonate dissolution via carbonic acid	open-system	< -10 ‰	Comparably low, i.e., around 10 %
	closed-system	> -10 ‰	Comparably high, i.e., close to 50 %
Carbonate dissolution via oxidation of pyrite		Close to 0 ‰	Very high, i.e., > 50 %
"Old" OM contribution to seepage water acidification		< -10 ‰	Shift towards higher values (> 50 % possible)

2011). The respective $\delta^{18}O$ values have been published earlier (Fohlmeister et al., 2013).

3.2 Radiocarbon analysis using LA-AMS

By focusing a laser on the surface of a solid sample at sufficiently high energy densities, a small portion of material is ablated and can be used for trace element or isotopic analysis allowing for fast and spatially resolved analysis (Gray, 1985; Koch and Gunther, 2011). ^{14}C analysis of SPA 127 was performed at the Laboratory of Ion Beam Physics, ETH Zurich, Switzerland, by LA coupled with AMS (Welte et al., 2016a, 2017). For this study, a slightly modified LA-AMS setup was used reaching a smaller spot size ($75 \times 140\,\mu m^2$) and higher energy densities of up to $8\,J/cm^2$ allowing for increased signal intensities, i.e., ^{12}C currents. With LA-AMS a quasi-continuous data stream is produced at 10 s intervals in the AMS. This is the minimal integration time of the AMS and together with the laser spot width d and the scanning velocity v defines the spatial resolution R according to $R = d + v \cdot 10\,s$.

LA scans were placed as close as possible to the stable isotope tracks in order to facilitate matching between the two data sets (Fig. 2). However, the LA-AMS setup does not permit laser tracks to be placed close to the rim of samples causing an offset between the two sampling lanes of approximately 5 mm. Speleothem growth layers are often curved, resulting in a potential offset between stable isotope and radiocarbon data of up to several hundred micrometers, with the outer LA scan appearing somewhat older than the stable isotope record. Since the curvature of the growth layers is most likely variable, a constant correction factor has not been applied.

On the "top piece" of SPA 127 two subsequent scans in opposite direction were performed, first from young to old (T1) and then vice versa (T2) on the same track with a scanning velocity of 20 µm/s and a laser energy density of approximately $5\,J/cm^2$. On the "bottom piece" a total of three analyses were performed: the initial scan from old to young (B1: 10 µm/s, 1–2 J/cm^2) was followed by a second repeated scan from bottom to top (B2: old to young, 25 µm/s, $8\,J/cm^2$) after removing the top ~ 0.5 mm of the sample surface by mechanical polishing. The second scan was necessary to ensure that the unusual ^{14}C signature observed in the oldest part of the stalagmite during the first scan (see Sect. 4) was not the result of a potentially contaminated surface. A final third analysis (B3) consisting of two scans performed in opposite directions was performed at 20 µm/s and $5\,J/cm^2$. Processing of the raw ^{14}C data was performed using in-house standards also analyzed by LA-AMS for blank subtraction and standard normalization (marble, $F^{14}C = 0$ and coral standard, $F^{14}C = 0.9445 \pm 0.0018$), and a conventional fractionation correction to $\delta^{13}C$ of -25 ‰ was applied (Stuiver and Polach, 1977). A Savitzky–Golay (SG) filter is applied to the recorded ^{14}C signal of B3, which is a smoothing method that reduces noise while maintaining the shape and height of peaks (Savitzky and Golay, 1964). In brief, a polynomial is fitted to a subset of the data points and evaluated at the center of the approximation interval. Two parameters, namely the number of points defining the approximation interval and the maximum polynomial order, can be defined. The smoothing has been applied to the two subscans of B3 (from "old to young" and vice versa) as well as to the combined data to ensure robustness of the filter. Corresponding uncertainties are estimated from the square root of the sum of the squared difference between the measured $F^{14}C$ value and the SG fit at each point within the interval. This value is then divided by the square root of the difference between the interval length (number of data points) and the maximum order allowed for the polynomial, which is equivalent to the degree of freedom.

4 Results

4.1 Dead carbon fraction

^{14}C results for both pieces of SPA 127 (T1, T2 and B3) are reported as dcf (blue line in Figs. 3a and S8a in the Supplement). Using the ^{14}C profile of the speleothem, the StalAge (Scholz and Hoffmann, 2011) age–depth model applied to previously published U–Th data (Fohlmeister et al., 2013) and the known ^{14}C content of the atmosphere during the Holocene (Reimer et al., 2016), the dcf was calculated according to Eq. (1) for the 1402 radiocarbon data points (Fig. 3a). A SG filter was applied (interval: 21, maximum polynomial order: 2), and for comparison the $\delta^{18}O$ and $\delta^{13}C$

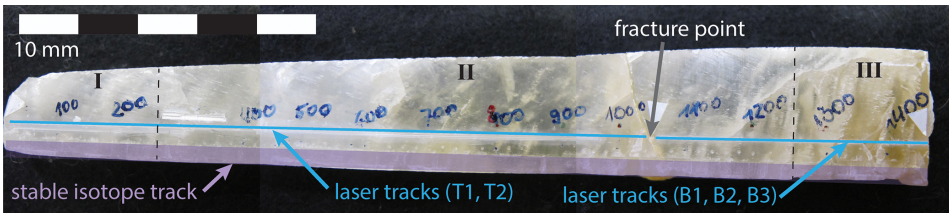

Figure 2. Polished slab of SPA 127 (top is left). The locations of the stable isotope track and of the LA-AMS tracks are marked in purple and blue, respectively. The total length of the slab is 14.6 cm. Roman numerals and dashed black lines mark the three sections discussed separately.

data are shown in the same graph (Fig. 3a and b). The U–Th dates and the corresponding average growth rate calculated using StalAge are displayed in Fig. 3c.

4.2 Stable C isotopes

The previously published $\delta^{18}O$ values (Fohlmeister et al., 2013) and unpublished $\delta^{13}C$ data (this study) are shown in Fig. 3a and b, respectively. A large amplitude and fast changes ranging from $-8\,‰$ to $+1\,‰$ characterize $\delta^{13}C$ throughout the entire length of the speleothem but are especially pronounced between 30 and 130 mm (ca. 4.0–8.1 ka). Layers exhibiting a comparably stable $\delta^{13}C$ occur at the top and bottom of SPA 127, specifically ranging from 4 to 25 mm (ca. 2.6 and 3.7 ka) and from 130 to 144 mm (ca. 8.1–8.4 ka).

5 Discussion

The interpretation of the results on C isotopes in SPA 127 will be divided into three sections that correspond to three sections identified on the speleothem based on their $\delta^{13}C$ characteristics, i.e., two periods of comparably stable $\delta^{13}C$ before 8 ka and after 3.5 ka and the interval in between with large and rapid fluctuations.

5.1 Old section of SPA 127 (8.5–8.0 ka)

In the oldest part of SPA 127, the dcf is comparably high ($\sim 60\,\%$), while $\delta^{13}C$ is relatively depleted with values lower than $-5\,‰$ on average. Although the reservoir effect is extremely high, in principle the obtained C-isotope composition can be explained without a major contribution of pyrite oxidation. The relatively low $\delta^{13}C$ value of $-5\,‰$ actually contradicts this mode of host rock dissolution but is in line with sparse C_3 vegetation ($\delta^{13}C \approx -25\,‰$) above the cave and host rock dissolution under nearly closed conditions (compare Fig. 4c and d). The stoichiometry of $CaCO_3$ dissolution by carbonic acid predicts that only about half of the C in the solution is derived from the host rock under nearly completely closed conditions. Given that the Jurassic host rock is devoid of ^{14}C, the biogenic component must be older than the contemporaneous atmosphere to allow dcf values greater than 50 %. Thus, in addition to the atmospheric radiocarbon contribution from living vegetation, an "old" OM source, which respires radiocarbon-depleted CO_2, is required to explain the depleted $\delta^{13}C$ values and elevated dcf. Such "old" OM is also argued to have contributed to the radiocarbon reservoir effect of Moomi Cave (Socotra Island) during the last glacial period (Therre et al., 2020). Observations from other cave and karst systems also point to important C pools deep in the vadose karst (e.g., Benavente et al., 2010; Bergel et al., 2017; Breecker et al., 2012). Nevertheless, in a sparsely vegetated high-elevation region this is the first finding of this kind.

The speleothem growth phase prior to 8.0 ka coincides with the early Holocene thermal maximum, which is also reflected by the depleted $\delta^{18}O$ values hinting towards higher temperatures (Fohlmeister et al., 2013; Mangini et al., 2005). Warmer periods likely favor microbial decomposition of, for example, OM present in the epikarst below the soil zone, which leads to an increase in pCO_2 and, hence, more acidic water. In turn, more $CaCO_3$ can be dissolved giving rise to higher speleothem growth rates, which is indeed observed in this period (Fig. 3, orange shaded area). Thus, the growth rate and the C-isotope composition of stalagmite SPA 127 are in agreement with the presence of a deep OM reservoir in the karst system above the cave.

5.2 Rapid changes in dcf and stable C isotopes (8.0 to 3.8 ka)

The growth rate was reduced in this period compared to the previous one (Fig. 3c). This either suggests that meteoric precipitation or the amount of soil-derived C were reduced, both resulting in a smaller amount of dissolved carbonate transported to the cave. The low $\delta^{13}C$ values of the first growth period were superseded by rapid and very large variations of $\delta^{13}C$. This pattern is complex and its interpretation is difficult, as this behavior has not been observed elsewhere. Processes in the soil and karst as well as in-cave processes must be considered. High-resolution LA-AMS ^{14}C measurements in conjunction with O isotope data and growth rate changes, however, greatly assist in disentangling the driving mechanism(s) for these $\delta^{13}C$ variations. The dcf between 8.0 and 3.8 ka is generally lower than in the older section. This means

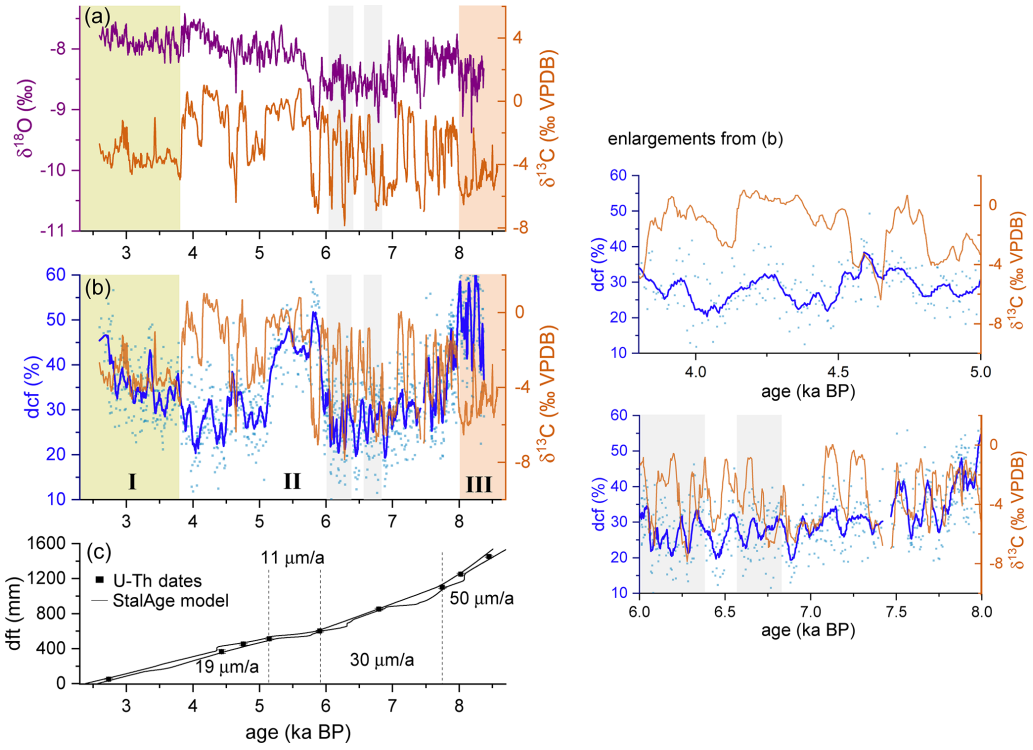

Figure 3. δ^{18}O represented by the purple line (Fohlmeister et al., 2013) compared to δ^{13}C (orange line) and **(b)** dcf (light blue dots) with a 21-point SG filter (dark blue line) plotted against age and compared to δ^{13}C. The yellow, white and orange shaded areas represent phases with distinct stable isotope characteristics. Roman numerals indicate the three subsections discussed in the text. Light grey shaded areas mark regions where the SG filter was determined with lower confidence. Enlargements of this graph are shown in the right panel. **(c)** Growth history of SPA 127 obtained by StalAge applied to dated depths (black squares, errors are smaller than the symbol size). Numbers represent average growth rates of the individual sections.

that either the aged OM in the karst was depleted or its degradation was reduced, possibly due to a reduction in meteoric precipitation (as deduced from growth rate reduction). Both reasons, less meteoric precipitation and a depleted deep OM pool, would explain well the observed reduction in growth rate. The only speleothem C sources available in this period were consequently the close-to-modern SOM and the radiocarbon-free host rock.

The dcf record shows a strong and rapid increase around 6 ka and a rapid decrease back to pre-6 ka levels at around 5 ka (Fig. 3b). The increase in dcf occurs at the same time as a significant decrease in δ^{18}O, but dcf remains elevated when δ^{18}O jumps back again shortly after. Instead, the decrease in dcf at 5 ka occurs contemporaneously with a δ^{13}C decrease after δ^{13}C values remained at elevated values for nearly a millennium. The reason for such a behavior of the dcf remains elusive. In this section, we focus on the cause of the large and rapid jumps in δ^{13}C by proposing two hypotheses.

Hypothesis 1: Processes above the cave, i.e., different carbonate dissolution processes, cause the rapid switching

Two different processes may have caused carbonate dissolution at Spannagel cave in this period. The first involves soil CO_2-derived carbonic acid (from root respiration and microbial decomposition of SOM) while the second process operates via sulfuric acid formed by pyrite oxidation (compare Fig. 4a and b). During times when the first process dominates, the stable carbon isotopic composition of stalagmites is strongly influenced by C from the soil shifting δ^{13}C towards more negative values. At the same time, the dcf is expected to be relatively low (at least $< 50\,\%$) as the comparably ^{14}C-rich soil C contributes significantly to the signal. In contrast, pyrite oxidation leads to more positive δ^{13}C values in the stalagmite corresponding to the δ^{13}C composition of the host rock, as the δ^{13}C-depleted biogenic source contributes little or even no C (Bajo et al., 2017; Spötl et al., 2016). Under these conditions, the dcf should increase to values close to 100 % if the comparably modern soil contribution is absent. If the observed δ^{13}C variations are caused by rapid alternation between both processes, a positive cor-

relation between $\delta^{13}C$ and the dcf has to be expected, with extreme values in the dcf as outlined above. However, no significant long-term positive correlation for the two data series, i.e., $\delta^{13}C$ and dcf, is observed (Fig. S10), and extreme dcf values are not observed. A robust comparison of both data sets is impeded because of the different spatial offset of the two measurement tracks from the growth axis. The radiocarbon track is located ca. 5 mm further from the central growth axis than the stable isotope track (Fig. 2). Growth layers cannot be identified, but the small stalagmite diameter suggests steeply dipping layers resulting in an apparent shift of the dcf towards older ages relative to $\delta^{13}C$. Indeed, such a delay is observable when comparing details in the two data series (Fig. 3b). Considering the potential offset between the two records (see Sect. 3), a high degree of similarity between main features in $\delta^{13}C$ and dcf are observable for the middle period, especially between 8 and 6 ka and also partly between 5 and 3.8 ka. Those phases are interrupted by the interval of the previously described strong increase in dcf.

The large swings in $\delta^{13}C$ suggest frequent switches between the carbonate dissolution mechanism from carbonic acid dissolution to pyrite oxidation. However, this is expected to be accompanied by an increase in the dcf to 100 % because of the diminishing ^{14}C-rich soil signature, which, however, is not observed. Generally, the dcf is even smaller than in the youngest and oldest sections of the stalagmite, i.e., after 3.8 ka and before 8 ka. Changes between open and closed carbonate dissolution regimes are expected to result in a positive relationship between the dcf and $\delta^{13}C$, which is observed in SPA 127. However, the magnitude of $\delta^{13}C$ variations is too large to be explained by a change of the dissolution regimes even when considering the extreme switch from completely open to completely closed (Hendy, 1971; Fohlmeister et al., 2011b). Thus, additional processes in the cave most likely caused this unusual behavior and the high-magnitude and high-frequency $\delta^{13}C$ variations.

Hypothesis 2: Processes in the cave cause the rapid switching

A major factor influencing the carbon isotope composition of stalagmites are fractionation processes (compare Fig. 4e and f), which occur during degassing of CO_2 and precipitation of $CaCO_3$ from the solution. Fast dripping results in fast growth and leaves less time for fractionation or C-isotope exchange (compare Fig. 4g and h) and vice versa (e.g., Fohlmeister et al., 2018; Scholz et al., 2009). In addition, the difference in pCO_2 between water and cave-air CO_2 can also influence isotope fractionation and C exchange processes. In the middle part of SPA 127, the average growth rate decreased to ≤ 30 µm/a, which is significantly lower than in the oldest section (50 µm/a). As discussed earlier, the reduction in growth rate might have been partly induced by reduced meteoric precipitation resulting in slower drip rates or by reduced soil or karst CO_2 concentrations leading to less dissolved host rock $CaCO_3$. In addition, a lower or absent contribution of an "old" OM reservoir in the karst would have led to a lower pCO_2 difference between the CO_2 concentration in the drip water and cave air, which favors an increase in $\delta^{13}C$ through C-isotope exchange processes in the cave. We hypothesize that the rapid changes in $\delta^{13}C$ might correlate with short-term changes in growth rate, which cannot be resolved by the available U–Th chronology, enabling or disabling isotope fractionation and C exchange between cave air CO_2 and DIC in drip water that are described in the following two paragraphs.

i. *Changes in isotope fractionation effects.* During periods of slow growth, fractionation processes can significantly alter the isotopic composition of the stalagmite. During CO_2 degassing from the drip water, the lighter molecules are preferentially transferred into the gas phase resulting in a solution enriched in heavy isotopes. Indeed, recent experiments (Fahrni et al., 2017) support earlier findings that fractionation of radiocarbon relative to ^{12}C is about twice as large as for ^{13}C relative to ^{12}C (Stuiver and Robinson, 1974). However, as radiocarbon measurements are corrected for fractionation effects via $\delta^{13}C$ values, it is impossible to detect a potential correlation between the two isotopes due to fractionation effects. However, potential fractionation affecting $\delta^{13}C$ also influences $\delta^{18}O$ and can be confirmed by a positive correlation between stable C isotopes and O isotopes (e.g., Dreybrodt, 2008; Polag et al., 2010). Applying a running correlation coefficient between $\delta^{13}C$ and $\delta^{18}O$ is a powerful tool to detect fractionation changes through time (Fohlmeister et al., 2017). The 11-point running correlation coefficients calculated for the two time series of SPA 127 show no stalagmite sections with a high correlation coefficient but vary without any obvious pattern between -1 and $+1$ (compare Fig. S10, bottom panel). Thus, fractionation was most likely not the main process causing the large variations in $\delta^{13}C$ but may have played a minor role during some periods.

ii. *Prior calcite precipitation (PCP).* PCP can have an effect on $\delta^{13}C$, even for a large stalagmite such as ours. While this would not have an effect on ^{14}C, we would expect that $\delta^{18}O$ should show a similar behavior, which is not the case (Fig. 3a). Thus, we can safely assume that PCP is not responsible for the rapid changes observed in SPA 127.

iii. *C exchange between cave air CO_2 and drip water DIC.* Another process that is a potential candidate for causing the behavior observed in SPA 127 in this interval is the C-isotope exchange between CO_2 of the cave air and C dissolved in the drip water. The C exchange between cave air CO_2 and DIC in drip water may be the dominant process if the stalagmite growth rate is suf-

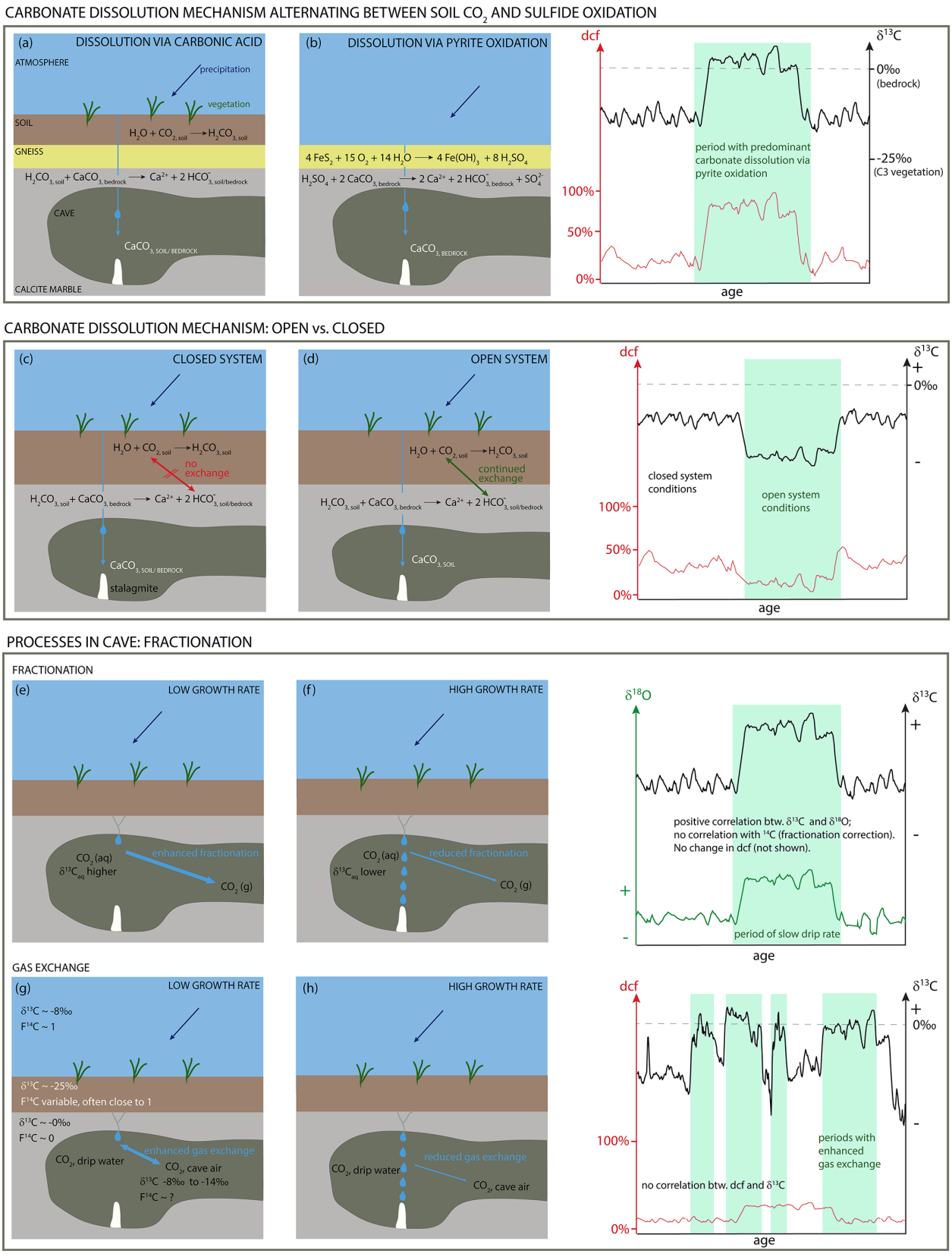

Figure 4. Overview of different processes that can influence $F^{14}C$ and $\delta^{13}C$ in speleothems. For details see text.

ficiently low and when drip interval is long, meaning that 95 % of the $CaCO_3$ precipitated either via PCP or on the stalagmite (Guo, 2020), and/or the differences between the pCO_2 of the water and cave air, is small (Hendy, 1971; Scholz et al., 2009). In this case, the C isotopic composition of the drip water when reaching the top of the stalagmite depends mainly on the initial $\delta^{13}C$ of drip water and on the degree of C-isotope exchange with the cave atmosphere. Spannagel Cave is well ventilated throughout the year with cave air $\delta^{13}C$ values of -10 ‰ to -11 ‰ (Tochterle et al., 2017), which is significantly lower than that of the atmosphere, i.e., approximately -8 ‰ (Keeling et al., 2010). These more negative values are a hint towards a contribution from soil air. The following assumptions were made: the $\delta^{13}C$ of drip water is composed of two biogenic C sources ($\delta^{13}C \sim -25$ ‰) and host rock ($\delta^{13}C \sim +2.8$ ‰) and about 20 %–30 % are derived from the host rock (based on the dcf in this interval). Accounting for about 10 ‰ to 11 ‰ fractionation between soil gas CO_2 and HCO_3^- during the transition of soil gas CO_2 to dissolved inorganic carbon (DIC), the initial drip water, which was feeding the stalagmite, had a $\delta^{13}C$ value between -11.5 ‰ and -9 ‰ (Mook et al., 1974). Considering Rayleigh fractionation effects in the cave, carbonate $\delta^{13}C$ values of -8 ‰ appear feasible (Scholz et al., 2009, Deininger et al., 2012) without any exchange of C isotopes. C-isotope exchange processes lead to water significantly enriched in ^{13}C. When cave air with $\delta^{13}C$ values around -11 ‰ exchanges with drip water, the C isotopic composition of the water will increase, as the transition of gaseous CO_2 to HCO_3^- involves a fractionation of about $+10$ ‰ to $+11$ ‰ at temperatures between 0 and 5° C (Mook et al., 1974). Thus, drip water in C isotopic equilibrium with cave air CO_2, which is the most extreme case, should have $\delta^{13}C$ values of -1 ‰ to 0 ‰. Precipitation of $CaCO_3$ from such water would result in $\delta^{13}C$ values of around 0 ‰ to $+1$ ‰ as observed for some short intervals.

Similar considerations can be applied to radiocarbon. If the cave ventilation is sluggish, $F^{14}C$ in the cave air will deviate from atmospheric values (i.e., $F^{14}C_{atm} \approx 1$) as it is influenced by other sources, such as soil air or CO_2 degassed from drip water, which are both depleted with respect to atmospheric values. In a recent study, cave air has been shown to be depleted in radiocarbon with values as low as $F^{14}C \approx 0.6$ (Minami et al., 2015). When the cave ventilation is not effectively changing the depleted radiocarbon towards more atmospheric values, C-isotope exchange processes are not detectable using ^{14}C in speleothems. As isotopic fractionation is not important for radiocarbon (as explained above), C-isotope exchange of DIC with cave air, which both have a similar radiocarbon content, would have no effect on the ^{14}C signal of the precipitated calcite.

5.3 Interpretation of dcf and $\delta^{13}C$ in the youngest section of SPA 127 (3.8 to 2.5 ka)

In the youngest section of this stalagmite a behavior similar to the oldest section with respect to $\delta^{13}C$ and radiocarbon content is observed. From approximately 3.8 ka onward, the dcf increases slowly from about 20 % to 50 %. Correspondingly, $\delta^{13}C$ shows a lower variability than in the middle part with mean $\delta^{13}C$ values of -3 ‰ to -4 ‰, which is also comparable to the behavior observed for the interval > 8 ka. As $\delta^{13}C$ does not show any long-term trend as observed for the reservoir effect, we rule out a change to more closed carbonate dissolution conditions driving the increase in dcf. The only explanation that can lead to such an increase is an "old" C reservoir. We propose that climatic conditions changed such that this "old" OM pool in the karst, which was decoupled from the atmosphere, has become the main OM-derived CO_2 source. This CO_2 resulted in acidification in a comparable way to soil CO_2 enhancing carbonate dissolution and ultimately contributed to stalagmite $CaCO_3$. The isotopic ^{14}C imprint, however, is significantly different to soil CO_2 causing the observed increase in dcf. Between approximately 8 and 6 ka the Alps experienced a warmer climate than today (Ivy-Ochs et al., 2009; Nicolussi et al., 2005). A study conducted by Nicolussi et al. (2005) in the Kauner valley, situated approximately 70 km west of Spannagel Cave, showed that the timberline was significantly higher during that period (Fig. 5) supporting a warmer climate. Between 6 and 4 ka the timberline was comparable to the present-day situation.

It is expected that with the lowering of the timberline after ~ 4 ka the vegetation density decreased as well, which should be reflected in the speleothem $\delta^{13}C$ values. This, however, is not the case during this period pointing towards a relatively stable contribution of soil-derived CO_2. Possibly, a certain proportion of plants that grew during the early to mid-Holocene warm epoch died and the corresponding OM located in the deeper vadose zone was initially stabilized due to reduced meteoric precipitation and later became mobilized due to enhanced microbial activity. Considering the low mean annual temperatures at this high-alpine site, decomposition processes are most likely slow, allowing OM to age during decomposition as indicated in a recent study by Shi et al. (2020). The radiocarbon composition of the aging SOM will closely follow a radiocarbon-specific exponential decay and is responsible for the depleted radiocarbon concentration in soil gas CO_2. Depending on the contribution of root-respired CO_2 of Alpine plants compared to the decomposed CO_2 from dead OM, the dcf will closely follow an exponential decay, resembling that of the radiocarbon decay, and thus would contribute to the observed increase in the dcf. The closer the observed increase in the dcf follows that of a radiocarbon decay trajectory, the larger the contri-

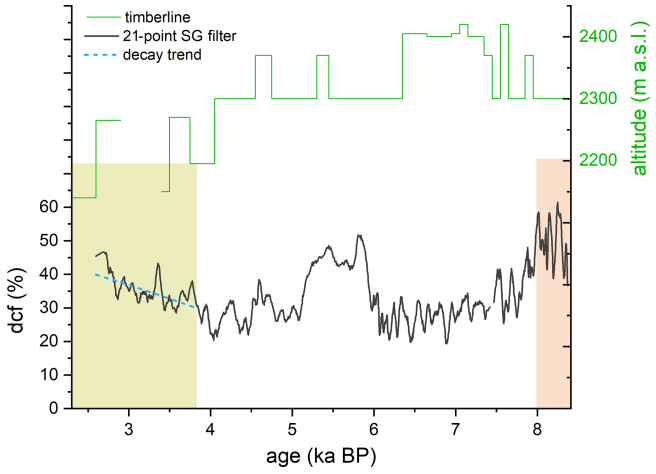

Figure 5. Comparison of the dcf in stalagmite SPA 127 with the elevation of the timberline reconstructed for the Kauner valley 70 km west of Spannagel Cave (green line, after Nicolussi et al., 2005) with the dcf. Around 4 ka the timberline started to decline, which is concurrent with an increase in dcf, i.e., a decrease in initial ^{14}C. This decrease closely follows a radiocarbon decay trend (dashed blue line). Green and red areas mark the three different time periods as indicated in Fig. 3.

bution of CO_2 from the aging SOM reservoir in relation to root-respired CO_2. Based on the observed rate of increase in dcf, which compares well with the radiocarbon decay trend (blue dashed line in Fig. 5), we suggest that the majority of DIC that contributed to the speleothem $CaCO_3$ had its origin in aged soil OM.

6 Conclusions

Combined stable carbon isotope and radiocarbon analyses of stalagmite SPA 127 provide a comprehensive picture of the carbon dynamics at Spannagel Cave. With the novel LA-AMS technique, a highly spatially resolved ^{14}C time series allows unprecedented insights into processes in this high-alpine karst system. Care has to be taken when applying LA-AMS to stalagmites as epoxy resin used in sample preparation leads to distorted results.

Results from this study allow three intervals with different carbon dynamics to be distinguished:

i. The interval before 8 ka is characterized by generally low and stable $\delta^{13}C$ values combined with a comparably high dcf ($> 50\,\%$) pointing towards the existence of an "old" OM reservoir in the epikarst. CO_2 emanating from this presaged C pool provides additional carbonic acid potentially enhancing bedrock dissolution.

ii. The interval between 8 and 3.8 ka is characterized by a strong variability in $\delta^{13}C$ with a generally lower dcf suggesting that the "old" OM reservoir in the karst had either been exhausted or stabilized (less production to aged respired soil/karst CO_2) possibly due to reduced meteoric precipitation. This is supported by a lower stalagmite growth rate in this period. C exchange between cave air CO_2 and DIC in drip water is the most likely explanation for the strong $\delta^{13}C$ variability, as (i) bedrock dissolution mechanisms, i.e., pyrite oxidation vs. carbonic acid dissolution, are not supported by the magnitude of changes in dcf and stable C, even though the temporal coherence indicates that some of the $\delta^{13}C$ variations might be explained by the bedrock dissolution mode (open vs. closed carbonate dissolution), and (ii) fractionation processes in the cave cannot explain the large shifts as no correlation between $\delta^{18}O$ and $\delta^{13}C$ is observed.

iii. In the interval between 3.8 and 2.4 ka the comparably more stable $\delta^{13}C$ signature combined with an increasing dcf hints towards a contribution from an aging OM reservoir in the karst similar to the period > 8 ka. This OM reservoir contributed to the stalagmite growth in this period due to warmer climatic conditions. While the contribution of "old" OM in the oldest growth phase was stable, the youngest section indicates an aging of this reservoir.

Data availability. The $\delta^{18}O$ and U-Th ages are published in Fohlmeister et al. (2013) and available on SISAL 2: https://doi.org/10.17864/1947.256 (Comas Bru et al., 2020).

Supplement. The supplement related to this article is available online at: https://doi.org/10.5194/cp-17-2165-2021-supplement.

Author contributions. CW, JF and CS conceptualized the content of this paper. CW, MW and BH carried LA-AMS measurements out, and CS conducted stable carbon isotope analyses. MW and LW developed the data reduction strategy. JF, CW and TE interpreted the data and compared them to published records. CW prepared the paper with contributions from all co-authors.

Competing interests. The authors declare that they have no conflict of interest.

Disclaimer. Publisher's note: Copernicus Publications remains neutral with regard to jurisdictional claims in published maps and institutional affiliations.

Acknowledgements. Jens Fohlmeister acknowledges support from DFG. Melina Wertnik was supported by ETH. FTIR analyses were performed by Laura Hendriks. We also thank the two reviewers who helped improve this paper.

Financial support. This research has been supported by the ETH Research Grant (grant no. ETH-03 18-2) and DFG (grant nos. FO 809/2-1 and FO 809/4-1).

Review statement. This paper was edited by Alberto Reyes and reviewed by two anonymous referees.

References

Bajo, P., Borsato, A., Drysdale, R., Hua, Q., Frisia, S., Zanchetta, G., Hellstrom, J., and Woodhead, J.: Stalagmite carbon isotopes and dead carbon proportion (DCP) in a near-closed-system situation: An interplay between sulphuric and carbonic acid dissolution, Geochim. Cosmochim. Ac., 210, 208–227, 2017.

Bar-Matthews, M., Ayalon, A., Kaufman, A., and Wasserburg, G. J.: The Eastern Mediterranean paleoclimate as a reflection of regional events: Soreq cave, Israel, Earth Planet Sc. Lett., 166, 85–95, 1999.

Benavente, J., Vadillo, I., Carrasco, F., Soler, A., Linan, C., and Moral, F.: Air Carbon Dioxide Contents in the Vadose Zone of a Mediterranean Karst, Vadose Zone J., 9, 126–136, 2010.

Bergel, S. J., Carlson, P. E., Larson, T. E., Wood, C. T., Johnson, K. R., Banner, J. L., and Breecker, D. O.: Constraining the subsoil carbon source to cave-air CO_2 and speleothem calcite in central Texas, Geochim. Cosmochim. Ac., 217, 112–127, 2017.

Breecker, D. O., Payne, A. E., Quade, J., Banner, J. L., Ball, C. E., Meyer, K. W., and Cowan, B. D.: The sources and sinks of CO_2 in caves under mixed woodland and grassland vegetation, Geochim. Cosmochim. Ac., 96, 230–246, 2012.

Cerling, T. E.: The Stable Isotopic Composition of Modern Soil Carbonate and Its Relationship to Climate, Earth Planet. Sc. Lett., 71, 229–240, 1984.

Cheng, H., Edwards, R. L., Shen, C.-C., Polyak, V. J., Asmerom, Y., Woodhead, J., Hellstrom, J., Wang, Y., Kong, X., and Spötl, C.: Improvements in 230Th dating, 230Th and 234U half-life values, and U–Th isotopic measurements by multi-collector inductively coupled plasma mass spectrometry, Earth Planet. Sc. Lett., 371, 82–91, 2013.

Cheng, H., Edwards, R. L., Sinha, A., Spotl, C., Yi, L., Chen, S., Kelly, M., Kathayat, G., Wang, X., Li, X., Kong, X., Wang, Y., Ning, Y., and Zhang, H.: The Asian monsoon over the past 640,000 years and ice age terminations, Nature, 534, 640–646, 2016.

Comas-Bru, L., Atsawawaranunt, K., Harrison, S., and SISAL working group members: SISAL (Speleothem Isotopes Synthesis and AnaLysis Working Group) database version 2.0, University of Reading [data set], https://doi.org/10.17864/1947.256, 2020.

Deininger, M., Fohlmeister, J., Scholz, D., and Mangini, A.: Isotope disequilibrium effects: The influence of evaporation and ventilation effects on the carbon and oxygen isotope composition of speleothems – A model approach, Geochim. Cosmochim. Ac., 96, 57–79, 2012.

Denniston, R. F., DuPree, M., Dorale, J. A., Asmerom, Y., Polyak, V. J., and Carpenter, S. J.: Episodes of late Holocene aridity recorded by stalagmites from Devil's Icebox Cave, central Missouri, USA, Quaternary Res., 68, 45–52, 2007.

Dreybrodt, W.: Evolution of the isotopic composition of carbon and oxygen in a calcite precipitating H_2O–CO_2–$CaCO_3$ solution and the related isotopic composition of calcite in stalagmites, Geochim. Cosmochim. Ac., 72, 4712–4724, 2008.

Fahrni, S. M., Southon, J. R., Santos, G. M., Palstra, S. W., Meijer, H. A., and Xu, X.: Reassessment of the 13C/12C and 14C/12C isotopic fractionation ratio and its impact on high-precision radiocarbon dating, Geochim. Cosmochim. Ac., 213, 330–345, 2017.

Fairchild, I. J. and Baker, A.: Speleothem science: from process to past environments, John Wiley & Sons, Oxford, 2012.

Fairchild, I. J., Smith, C. L., Baker, A., Fuller, L., Spotl, C., Mattey, D., McDermott, F., and Eimp: Modification and preservation of environmental signals in speleothems, Earth-Sci. Rev., 75, 105–153, 2006.

Fohlmeister, J., Schroder-Ritzrau, A., Spotl, C., Frisia, S., Miorandi, R., Kromer, B., and Mangini, A.: The Influences of Hydrology on the Radiogenic and Stable Carbon Isotope Composition of Cave Drip Water, Grotta Di Ernesto (Italy), Radiocarbon, 52, 1529–1544, 2010a.

Fohlmeister, J., Schroeder-Ritzrau, A., Spoetl, C., Frisia, S., Miorandi, R., Kromer, B., and Mangini, A.: The influences of hydrology on the radiovenic and stable carbon isotope composition of cave drip water, Grotta die Ernesto (Italy), Radiocarbon, 52, 1529–1544, 2010b.

Fohlmeister, J., Kromer, B., and Mangini, A.: The Influence of Soil Organic Matter Age Spectrum on the Reconstruction of Atmospheric C-14 Levels Via Stalagmites, Radiocarbon, 53, 99–115, 2011a.

Fohlmeister, J., Scholz, D., Kromer, B., and Mangini, A.: Modelling carbon isotopes of carbonates in cave drip water, Geochim. Cosmochim. Ac., 75, 5219–5228, 2011b.

Fohlmeister, J., Vollweiler, N., Spotl, C., and Mangini, A.: COMNISPA II: Update of a mid-European isotope climate record, 11 ka to present, Holocene, 23, 749–754, 2013.

Fohlmeister, J., Plessen, B., Dudashvili, A. S., Tjallingii, R., Wolff, C., Gafurov, A., and Cheng, H.: Winter precipitation changes during the Medieval Climate Anomaly and the Little Ice Age in arid Central Asia, Quaternary Sci. Rev., 178, 24–36, 2017.

Fohlmeister, J., Arps, J., Spotl, C., Schroder-Ritzrau, A., Plessen, B., Gunter, C., Frank, N., and Trussel, M.: Carbon and oxygen isotope fractionation in the water-calcite-aragonite system, Geochim. Cosmochim. Ac., 235, 127–139, 2018.

Fohlmeister, J., Voarintsoa, N. R. G., Lechleitner, F. A., Boyd, M., Brandtstatter, S., Jacobson, M. J., and Oster, J. L.: Main controls on the stable carbon isotope composition of speleothems, Geochim. Cosmochim. Ac., 279, 67–87, 2020.

Genty, D. and Massault, M.: Bomb C-14 recorded in laminated speleothems: Calculation of dead carbon proportion, Radiocarbon, 39, 33–48, 1997.

Gray, A. L.: Solid Sample Introduction by Laser Ablation for Inductively Coupled Plasma Source-Mass Spectrometry, Analyst, 110, 551–556, 1985.

Griffiths, M. L., Fohlmeister, J., Drysdale, R. N., Hua, Q., Johnson, K. R., Hellstrom, J. C., Gagan, M. K., and Zhao, J. X.: Hydrological control of the dead carbon fraction in a Holocene tropical speleothem, Quat. Geochronol., 14, 81–93, 2012.

Guo, W.: Kinetic clumped isotope fractionation in the DIC-H2O-CO2 system: Patterns, controls, and implications, Geochim. Cosmochim. Ac., 268, 230–257, 2020.

Hendy, C. H.: The isotopic geochemistry of speleothems – I. The calculation of the effects of different modes of formation on the isotopic composition of speleothems and their applicability as palaeoclimatic indicators, Geochim. Cosmochim. Ac., 35, 801–824, 1971.

Ivy-Ochs, S., Kerschner, H., Maisch, M., Christl, M., Kubik, P. W., and Schluchter, C.: Latest Pleistocene and Holocene glacier variations in the European Alps, Quaternary Sci. Rev., 28, 2137–2149, 2009.

Keeling, R., Piper, S., Bollenbacher, A., and Walker, S.: Monthly atmospheric 13C/12C isotopic ratios for 11 SIO stations, in: Trends: a compendium of data on global change, Carbon Dioxide Information Analysis Center, Oak Ridge Na- tional Laboratory, U.S. Department of Energy, Oak Ridge, Tenn., USA, 2010.

Koch, J. and Gunther, D.: Review of the state-of-the-art of laser ablation inductively coupled plasma mass spectrometry, Appl. Spectrosc., 65, 155–162, 2011.

Kutschera, W.: Applications of accelerator mass spectrometry, Int. J. Mass Spectrom., 349, 203–218, 2013.

Lachniet, M. S.: Climatic and environmental controls on speleothem oxygen-isotope values, Quaternary Sci. Rev., 28, 412–432, 2009.

Lauritzen, S.-E.: Marble stripe karst of the Scandinavian Caledonides: an end-member in the contact karst spectrum, Slovenska akademija znanosti in umetnosti, Acta Carsologica, 30, 47–79, 2001.

Lechleitner, F. A., Baldini, J. U. L., Breitenbach, S. F. M., Fohlmeister, J., McIntyre, C., Goswami, B., Jamieson, R. A., van der Voort, T. S., Prufer, K., Marwan, N., Culleton, B. J., Kennett, D. J., Asmerom, Y., Polyak, V., and Eglinton, T. I.: Hydrological and climatological controls on radiocarbon concentrations in a tropical stalagmite, Geochim. Cosmochim. Ac., 194, 233–252, 2016.

Mangini, A., Spötl, C., and Verdes, P.: Reconstruction of temperature in the Central Alps during the past 2000 yr from a δ18O stalagmite record, Earth Planet. Sc. Lett., 235, 741–751, 2005.

Mattey, D. P., Atkinson, T. C., Barker, J. A., Fisher, R., Latin, J. P., Durrell, R., and Ainsworth, M.: Carbon dioxide, ground air and carbon cycling in Gibraltar karst, Geochim. Cosmochim. Ac., 184, 88–113, 2016.

Minami, M., Kato, T., Horikawa, K., and Nakamura, T.: Seasonal variations of 14C and δ13C for cave drip waters in Ryugashi Cave, Shizuoka Prefecture, central Japan, Nucl. Instrum. Meth. B, 362, 202–209, 2015.

Mook, W. G., Bommerson, J. C., and Staverman, W. H.: Carbon Isotope Fractionation between Dissolved Bicarbonate and Gaseous Carbon-Dioxide, Earth Planet. Sc. Lett., 22, 169–176, 1974.

Moseley, G. E., Spötl, C., Brandstätter, S., Erhardt, T., Luetscher, M., and Edwards, R. L.: NALPS19: sub-orbital-scale climate variability recorded in northern Alpine speleothems during the last glacial period, Clim. Past, 16, 29–50, https://doi.org/10.5194/cp-16-29-2020, 2020.

Nicolussi, K., Kaufmann, M., Patzelt, G., van der Plicht, J., and Thurner, A.: Holocene tree-line variability in the Kauner Valley, Central Eastern Alps, indicated by dendrochronological analysis of living trees and subfossil logs, Veg. Hist. Archaeobot., 14, 221–234, 2005.

Noronha, A. L., Johnson, K. R., Hu, C. Y., Ruan, J. Y., Southon, J. R., and Ferguson, J. E.: Assessing influences on speleothem dead carbon variability over the Holocene: Implications for speleothem-based radiocarbon calibration, Earth Planet. Sc. Lett., 394, 20–29, 2014.

Noronha, A. L., Johnson, K. R., Southon, J. R., Hu, C. Y., Ruan, J. Y., and McCabe-Glynn, S.: Radiocarbon evidence for decomposition of aged organic matter in the vadose zone as the main source of speleothem carbon, Quaternary Sci. Rev., 127, 37–47, 2015.

Polag, D., Scholz, D., Muhlinghaus, C., Spotl, C., Schroder-Ritzrau, A., Segl, M., and Mangini, A.: Stable isotope fractionation in speleothems: Laboratory experiments, Chem. Geol., 279, 31–39, 2010.

Reimer, P. J., Bard, E., Bayliss, A., Beck, J. W., Blackwell, P. G., Ramsey, C. B., Buck, C. E., Cheng, H., Edwards, R. L., Friedrich, M., Grootes, P. M., Guilderson, T. P., Haflidason, H., Hajdas, I., Hatté, C., Heaton, T. J., Hoffmann, D. L., Hogg, A. G., Hughen, K. A., Kaiser, K. F., Kromer, B., Manning, S. W., Niu, M., Reimer, R. W., Richards, D. A., Scott, E. M., Southon, J. R., Staff, R. A., Turney, C. S. M., and van der Plicht, J.: IntCal13 and Marine13 Radiocarbon Age Calibration Curves 0–50,000 Years cal BP, Radiocarbon, 55, 1869–1887, 2016.

Richards, D. A. and Dorale, J. A.: Uranium-series chronology and environmental applications of speleothems, Rev. Mineral. Geochem., 52, 407–460, 2003.

Savitzky, A. and Golay, M. J. E.: Smoothing + Differentiation of Data by Simplified Least Squares Procedures, Anal. Chem., 36, 1627–1639, 1964.

Scholz, D. and Hoffmann, D.: ^{230}Th/U-dating of fossil reef corals and speleothems, Quaternary Sci. J., 57, 52–77, 2008.

Scholz, D. and Hoffmann, D. L.: StalAge – An algorithm designed for construction of speleothem age models, Quat. Geochronol., 6, 369–382, 2011.

Scholz, D., Mühlinghaus, C., and Mangini, A.: Modelling δ13C and δ18O in the solution layer on stalagmite surfaces, Geochim. Cosmochim. Ac., 73, 2592–2602, 2009.

Shi, Z., Allison, S. D., He, Y. J., Levine, P. A., Hoyt, A. M., Beem-Miller, J., Zhu, Q., Wieder, W. R., Trumbore, S., and Randerson, J. T.: The age distribution of global soil carbon inferred from radiocarbon measurements, Nat. Geosci., 13, 555–559, 2020.

Southon, J., Noronha, A. L., Cheng, H., Edwards, R. L., and Wang, Y.: A high-resolution record of atmospheric 14C based on Hulu Cave speleothem H82, Quaternary Sci. Rev., 33, 32–41, 2012.

Spötl, C.: Long-term performance of the Gasbench isotope ratio mass spectrometry system for the stable isotope analysis of carbonate microsamples, Rapid Commun. Mass Spectrom., 25, 1683–1685, 2011.

Spötl, C. and Mangini, A.: Speleothems and paleoglaciers, Earth Planet. Sc. Lett., 254, 323–331, 2007.

Spötl, C. and Mangini, A.: Paleohydrology of a high-elecation, glacier influenced karst system in the central alps (Austria), Austrian J. Earth Sci., 103, 92–105, 2010.

Spötl, C. and Mattey, D.: Stable isotope microsampling of speleothems for palaeoenvironmental studies: A comparison of microdrill, micromill and laser ablation techniques, Chem. Geol., 235, 48–58, 2006.

Spötl, C., Mangini, A., Bums, S. J., Frank, N., and Pavuza, R.: Speleothems from the high-alpine Spannagel cave, Zillertal Alps (Austria), in: Studies of cave sediments, Springer, New York, 2004.

Spötl, C., Fairchild, I. J., and Tooth, A. F.: Cave air control on dripwater geochemistry, Obir Caves (Austria): Implications for speleothem deposition in dynamically ventilated caves, Geochim. Cosmochim. Ac., 69, 2451–2468, 2005.

Spötl, C., Fohlmeister, J., Cheng, H., and Boch, R.: Modern aragonite formation at near-freezing conditions in an alpine cave, Carnic Alps, Austria, Chem. Geol., 435, 60–70, 2016.

Stuiver, M. and Polach, H. A.: Reporting of C-14 Data – Discussion, Radiocarbon, 19, 355–363, 1977.

Stuiver, M. and Robinson, S. W.: University of Washington GEOSECS north Atlantic carbon-14 results, Earth Planet. Sc. Lett., 23, 87–90, 1974.

Therre, S., Fohlmeister, J., Fleitmann, D., Matter, A., Burns, S. J., Arps, J., Schröder-Ritzrau, A., Friedrich, R., and Frank, N.: Climate-induced speleothem radiocarbon variability on Socotra Island from the Last Glacial Maximum to the Younger Dryas, Clim. Past, 16, 409–421, https://doi.org/10.5194/cp-16-409-2020, 2020.

Tochterle, P., Dublyansky, Y., Stobener, N., Mandic, M., and Spotl, C.: High-resolution isotopic monitoring of cave air CO_2, Rapid Commun. Mass Spectrom., 31, 895–900, 2017.

Trumbore, S.: Age of soil organic matter and soil respiration: Radiocarbon constraints on belowground C dynamics, Ecol. Appl., 10, 399–411, 2000.

Wackerbarth, A., Scholz, D., Fohlmeister, J., and Mangini, A.: Modelling the δ18O value of cave drip water and speleothem calcite, Earth Planet. Sc. Lett., 299, 387–397, 2010.

Welte, C., Wacker, L., Hattendorf, B., Christl, M., Fohlmeister, J., Breitenbach, S. F., Robinson, L. F., Andrews, A. H., Freiwald, A., and Farmer, J. R.: Laser Ablation–Accelerator Mass Spectrometry: An Approach for Rapid Radiocarbon Analyses of Carbonate Archives at High Spatial Resolution, Anal. Chem., 88, 8570–8576, 2016a.

Welte, C., Wacker, L., Hattendorf, B., Christl, M., Koch, J., Synal, H. A., and Gunther, D.: Novel Laser Ablation Sampling Device for the Rapid Radiocarbon Analysis of Carbonate Samples by Accelerator Mass Spectrometry, Radiocarbon, 58, 419–435, 2016b.

Welte, C., Wacker, L., Hattendorf, B., Christl, M., Koch, J., Yeman, C., Breitenbach, S. F. M., Synal, H. A., and Gunther, D.: Optimizing the analyte introduction for C-14 laser ablation-AMS, J. Anal. Atom. Spectrom., 32, 1813–1819, 2017.

Yeman, C., Christl, M., Hattendorf, B., Wacker, L., Welte, C., Brehm, N., and Synal, H. A.: Unravelling Quasi-Continuous 14C Profiles by Laser Ablation AMS, Radiocarbon, 62, 453–465, 2019.